J Membrane Biol (2008) 221:61–72
DOI 10.1007/s00232-007-9078-0

Ca^{2+}-Induced Cl^- Efflux at Rat Distal Colonic Epithelium

B. Hennig · G. Schultheiss · K. Kunzelmann · M. Diener

Received: 26 March 2007 / Accepted: 8 October 2007 / Published online: 24 January 2008

Abstract With the aid of the halide-sensitive dye 6-methoxy-*N*-ethylquinolinium iodide (MEQ), changes in intracellular Cl^- concentration were measured to characterize the role of Ca^{2+}-dependent Cl^- channels at the rat distal colon. In order to avoid indirect effects of secretagogues mediated by changes in the driving force for Cl^- exit (i.e., mediated by opening of Ca^{2+}-dependent K^+ channels), all experiments were performed under depolarized conditions, i.e., in the presence of high extracellular K^+ concentrations. The Ca^{2+}-dependent secretagogue carbachol induced a stilbene-sensitive Cl^- efflux, which was mimicked by the Ca^{2+} ionophore ionomycin. Surprisingly, the activation of Ca^{2+}-dependent Cl^- efflux was resistant against blockers of classical Ca^{2+} signaling pathways such as phospholipase C, protein kinase C and calmodulin. Hence, alternative pathways must be involved in the signaling cascade. One possible signaling molecule seems to be nitric oxide (NO) as the NO donor sodium nitroprusside could induce Cl^- efflux. Vice versa, the NO synthase inhibitor *N*-ω-monomethyl-arginine (L-NMMA) reduced the carbachol-induced Cl^- efflux. This indicates that NO may be involved in part of the signaling cascade. In order to test the ability of the epithelium to produce NO, the expression of different isoforms of NO synthase was verified by immunohistochemistry. In addition, the cytoskeleton seems to play a role in the activation of Ca^{2+}-dependent Cl^- channels. Inhibitors of microtubule association such as nocodazole and colchicine as well as jasplakinolide, a drug that enhances actin polymerization, inhibited the carbachol-induced Cl^- efflux. Consequently, the activation of apical Cl^- channels by muscarinic receptor stimulation differs in signal transduction from the classical phospholipase C/protein kinase C way.

Keywords Anion secretion · Bestrophin · Ca^{2+} · Cl^- conductance · Cytoskeleton · Nitric oxide · Rat distal colon

B. Hennig · G. Schultheiss · M. Diener (✉)
Institut für Veterinär-Physiologie, Frankfurter Str. 100,
D-35392 Giessen, Germany
e-mail: martin.diener@vetmed.uni-giessen.de

K. Kunzelmann
Institut für Physiologie, Universitätsstr. 31,
D-93053 Regensburg, Germany

Introduction

Apical Cl^- channels are centrally involved in intestinal Cl^- secretion. The dominant intestinal apical Cl^- channel is the cystic fibrosis transmembrane regulator (CFTR) channel (Greger, 2000), which seems to carry most of the Cl^-carried short-circuit current (I_{sc}) after stimulation with secretagogues at many epithelia including the rat distal colon (Strabel & Diener, 1995). In this tissue, an increase in the intracellular concentration of cyclic adenosine monophosphate (cAMP) or Ca^{2+} induces a switch from electrolyte absorption into the secretion predominantly of Cl^- ions (Binder & Sandle, 1994). The predominant mechanism of its activation consists in the protein kinase A-dependent phosphorylation after an increase in the intracellular cAMP concentration (*for review*, *see* Jentsch et al., 2002). In contrast, the predominant effect of an increase in the cytosolic Ca^{2+} concentration consists in the opening of basolateral (Böhme, Diener & Rummel, 1991) and apical (Schultheiss et al., 2003) Ca^{2+}-dependent K^+ channels, which evokes a hyperpolarization of the membrane and thereby increases the driving force for Cl^- efflux across the dominant apical CFTR conductance.

However, when the action of Ca^{2+}-dependent agonists such as the cholinergic derivative carbachol on Ca^{2+}-dependent K^+ channels is passed by the use of high K^+ buffers (driving a Cl^- current across the apical membrane by a serosally to mucosally oriented Cl^- concentration gradient), the transient activation of a Ca^{2+}-dependent, stilbene-sensitive Cl^- conductance can be observed at the rat distal colon (Schultheiss, Siefjediers & Diener, 2005), which is followed by long-lasting inhibition of the apical, CFTR-mediated Cl^- conductance observed earlier (*see, e.g.*, Warhurst al., 1991; Barrett et al., 1998; Schultheiss, Ribeiro & Diener, 2001). The mechanism of activation of this Ca^{2+}-dependent Cl^- efflux pathway is only scarcely characterized. In addition, nothing is known about the localization of this conductance, i.e., the question of whether all cells along the crypt axis express this efflux pathway. Therefore, in the present study, changes in intracellular Cl^- concentration evoked by carbachol were tested under depolarized conditions in order to rule out indirect effects via opening of K^+ channels, at crypts loaded with the halide-sensitive dye 6-methoxy-*N*-ethylquinolinium iodide (MEQ).

Materials and Methods

Solutions

For the experiments carried out with isolated crypts, the following buffers were used. The ethylenediaminetetraacetic acid (EDTA) solution for the isolation contained (mmol $\cdot$ l^{-1}) NaCl 107, KCl 4.5, $NaHCO_3$ 25, Na_2HPO_4 1.8, NaH_2PO_4 0.2, glucose 12.2 and EDTA 10 plus 1 g $\cdot$ l^{-1} bovine serum albumin (BSA). It was gassed with carbogen (95% O_2, 5% CO_2, v/v); pH was adjusted by tris (hydroxymethyl)-aminomethane (TRIS) base to 7.4. The isolated crypts were stored in a high-potassium Tyrode solution consisting of (mmol$\cdot l^{-1}$) K gluconate 100, KCl 30, 4-(2-hydroxyethyl)-1-piperazineethanesulfonic acid (HEPES) 10, NaCl 20, $MgCl_2$ 1, $CaCl_2$ 1.25, glucose 12.2 and Na pyruvate 5 plus 1 g $\cdot$ l^{-1} BSA; pH was 7.4.

Each experiment with isolated crypts loaded with the halide-sensitive dye MEQ was started by superfusion with NaCl Tyrode solution containing (mmol $\cdot$ l^{-1}) NaCl 140, KCl 5.4, HEPES 10, glucose 12.2, $CaCl_2$ 1.25 and $MgCl_2$ 1. Thereafter, the membranes of the crypt cells were depolarized by replacing NaCl with equimolar KCl. Subsequently, a Cl^- efflux was induced by replacing the KCl by an equimolar K gluconate solution. The pH of all these solutions was adjusted to 7.4.

To calibrate the MEQ fluorescence signal, the intracellular Cl^- concentration was first clamped to values near zero by superfusion with the 140 mmol $\cdot$ l^{-1} K gluconate Tyrode. This was followed by superfusion with a solution of intermediate Cl^- concentration (101 mmol $\cdot$ l^{-1} K gluconate/39 mmol $\cdot$ l^{-1} KCl). The ionophores tributyltin (a Cl^-/OH^- ionophore, 8 $\cdot$ 10^{-6} mol $\cdot$ l^{-1}) and nigericin (a K^+/H^+ ionophore, 5 $\cdot$ 10^{-6} mol $\cdot$ l^{-1}) were added to these solutions to increase the Cl^- permeability of the cell membrane (MacVinnish, Reancharoen & Cuthbert, 1993). Finally, the MEQ fluorescence signal was completely quenched by a 140 mmol $\cdot$ l^{-1} KSCN solution containing (mmol$\cdot l^{-1}$) KSCN 140, HEPES 10, glucose 12.2, $CaCl_2$ 1.25 and $MgCl_2$ 1; pH was 7.4. Valinomycin (5 $\cdot$ 10^{-6} mol $\cdot$ l^{-1}) was added to this buffer in order to avoid negative charging of the cells provoked by SCN^- influx.

All Ussing chamber experiments started in a bathing solution containing (mmol $\cdot$ l^{-1}) NaCl 107, KCl 4.5, $NaHCO_3$ 25, Na_2HPO_4 0.2, $CaCl_2$ 1.25, $MgSO_4$ 1 and glucose 12.2. The buffer for the depolarization of the basolateral membrane contained (mmol $\cdot$ l^{-1}) KCl 111.5, $NaHCO_3$ 25, Na_2HPO_4 0.2, $CaCl_2$ 1.25, $MgSO_4$ 1 and glucose 12.2. In order to obtain a serosal-to-mucosal Cl^- gradient, 107 mmol $\cdot$ l^{-1} of Cl^- (in the form of KCl) of this buffer solution was replaced equimolarly by the impermeable anion gluconate in the apical bathing solution, thus containing (mmol $\cdot$ l^{-1}) K gluconate 107, KCl 4.5, $NaHCO_3$ 25, Na_2HPO_4 0.2, $CaCl_2$ 1.25, $MgSO_4$ 1 and glucose 12.2. All solutions were gassed with a mixture of 5% CO_2 and 95% O_2 (v/v); pH was 7.4.

For immunhistochemical experiments, a 100 mmol $\cdot$ l^{-1} phosphate buffer was used containing 80 mmol $\cdot$ l^{-1} Na_2HPO_4 and 20 mmol $\cdot$ l^{-1} NaH_2PO_4; pH was 7.4. 4′,6-Diamidino-2-phenylindole (DAPI) was dissolved in a phosphate-buffered saline (PBS) solution containing (in mmol $\cdot$ l^{-1}) sodium phosphate buffer 10, NaCl 120 and KCl 2.7; pH was 7.4.

Tissue Preparation

All experiments were performed with Wistar rats. Rats used for Ussing chamber experiments weighed 180–200 g; rats used for MEQ experiments weighed 120–150 g. All animals had free access to water and food until the day of the experiment. Animals were killed by a blow on the head, followed by exsanguination (approved by Regierungspräsidium Giessen, Giessen, Germany). The colon was placed on a small plastic rod with a diameter of 5 mm. Then, a circular incision was made near the anal end with a blunt scalpel, and the serosa as well as the muscularis propria were gently removed in a proximal direction. Thus, a mucosa–submucosa preparation was obtained.

Crypt Isolation and MEQ Experiments

For the isolation of intact crypts, one segment of the mucosa–submucosa preparation (1.5 cm wide, 3 cm long) was fixed on

a plastic holder with tissue adhesive and transferred for about 6–7 min in the EDTA solution. Afterward, the mucosa was vibrated once for about 30 s in order to obtain crypts. They were collected in high-potassium Tyrode buffer (Böhme et al., 1991). Changes of intracellular Cl^- concentration were measured with the halide-sensitive dye MEQ. Therefore, isolated crypts were fixed on a coverslip by dint of poly-L-lysine (0.1 g · l^{-1}). As MEQ itself is not cell-permeable, the reduced form, 6-methoxy-*N*-ethyl-1,2-dihydroquinoline (DiH-MEQ) had to be synthesized (*for details, see* Biwersi & Verkman, 1991). The isolated crypts fixed on the coverslips were loaded with DiH-MEQ ($4 \cdot 10^{-4}$ mol · l^{-1}) for 15 min at 37°C. Thereafter, the dye was washed away twice and the crypts were kept at 37°C for another 15 min. During this time, DiH-MEQ was reoxidized by the cells. Then, the coverslips were fixed in the experimental chambers with a volume of 3 ml. During the experiments, the crypts were superfused by the solutions described above with a perfusion rate of 1.5 ml · min^{-1}.

Experiments were carried out on an inverted microscope (IX-50; Olympus, Tokyo, Japan) equipped with an epifluorescence setup and an image analysis system (Till Photonics, Martinsried, Germany). Cells were excited at 344 nm, and the emission above 410 nm was measured from several regions of interest. Data were sampled with 0.1 Hz. The baseline was measured for several minutes before changing the bath solution or administering the drugs.

Short-Circuit Current Measurements

The tissue was mounted in a modified Ussing chamber, bathed with a volume of 3.5 ml on each side of the mucosa and short-circuited by a computer-controlled voltage-clamp device (Ingenieur Büro für Mess- und Datentechnik Mussler, Aachen, Germany) with correction for solution resistance. The exposed surface of the tissue was 1 cm^2. Short-circuit current (I_{sc}) was continuously recorded, and tissue conductance (G_t) was measured every minute. I_{sc} is expressed as μEq · h^{-1} · cm^{-2}, i.e., the flux of a monovalent ion per time and area, with 1 μEq · h^{-1} · cm^{-2} = 26.9 μA · cm^{-2}. Tissues were left for about 1 h to stabilize I_{sc} in standard 107 mmol · l^{-1} NaCl buffer solution (*see above*) before the basolateral membrane was depolarized with the KCl 111.5 mmol · l^{-1} buffer. Due to the high basolateral K^+ permeability, the electrical properties of the tissue, which are normally characterized by two batteries in series, are then expected to be dominated by the apical membrane (Fuchs, Larsen & Lindemann, 1977). After stabilization of I_{sc}, a Cl^- current across the apical membrane was driven by administration of the 107 mmol · l^{-1} K gluconate buffer at the mucosal side (Schultheiss et al., 2005). The baseline in electrical parameters was determined as mean over 3 min just before administration of a drug.

Immunohistochemistry

The tissue was rinsed with phosphate buffer and embedded in gelatin (gelatin type A from porcine skin, 100 g · l^{-1}). Then, the tissue was cryofixed in N_2-cooled 2-methylbutane. Sections (16 μm thick) were cut and mounted on glass slides coated with gelatin containing chrome alum (chromium[III] potassium sulfate, 0.5 g · l^{-1}).

Immunohistochemical staining was performed using the indirect immunofluorescence technique. After rehydration in phosphate buffer, the sections were incubated in phosphate buffer containing 2 ml · l^{-1} Triton-X-100, 30 g · l^{-1} BSA and 100 ml · l^{-1} goat serum (Chemicon, Temecula, CA) to block unspecific binding. Then, the blocking solution was removed and the sections were incubated with the respective primary antibody against NOS-1 (Becton Dickinson, Heidelberg, Germany; rabbit polyclonal antibody against human NOS-1 amino acids 1095–1289, final dilution 1:800), NOS-2 (Chemicon, Hofheim, Germany; rabbit polyclonal antibody against NOS-2 murine C-terminal peptide, final dilution 1:200), NOS-3 (Chemicon, Hofheim, Germany; rabbit polyclonal antibody against human NOS-3 amino acids 596–610, final dilution 1:800) or bestrophin 1 (affinity-purified rabbit anti-mouse polyclonal antibody, final dilution 1:1,000; Puntheeranurak et al., 2007) for 36 h at 4°C.

The antibody was dissolved in phosphate buffer containing 1 ml · l^{-1} Triton-X-100, 5 g · l^{-1} milk powder, 10 g · l^{-1} BSA and 10 ml · l^{-1} goat serum. After rinsing with phosphate buffer, the sections were incubated with the secondary antibody ($Cy3^{TM}$-conjugated affinipure donkey anti-rabbit immunoglobulin G, working dilution 1:800; Dianova, Hamburg, Germany) for 1 h at room temperature. After a further rinse with phosphate buffer, the sections were incubated for 5 min with $3 \cdot 10^{-7}$ mol · l^{-1} DAPI (Molecular Probes, Leiden, The Netherlands) dissolved in PBS. As negative control, some sections were incubated with a solution that did not contain the primary antibodies (*see* Fig. 6 rows 2, 4 and 6).

The preparations were examined on a fluorescence microscope (Nikon, Düsseldorf, Germany; 80i). Digital images were taken with a B/W camera (DS-2M B/Wc) using NIS Elements 2.30 software (all from Nikon) to finally adjust brightness, color and contrast.

Drugs

Calmidazolium, cytochalasin D, 4,4'-diisothiocyanatostilbene-2,2'-disulfonic acid disodium salt (DIDS), glibenclamide, 2-[1-(3-dimethylpropyl)-5-methoxy-indol-3-yl]-3-(1H-indol-3-yl)maleimide (Gö 6983; Calbiochem, Bad Soden, Germany), nocodazole and staurosporine were

dissolved in dimethylsulfoxide (DMSO). Colchicine, N-ω-monomethyl-arginine (L-NMMA; Tocris Cookson, Bristol, UK), 4-scetamido-4'-isothiocyanato-stilbene-2,2'-disulfonic acid sodium salt (SITS; Calbiochem) and sodium nitroprusside (SNP) were dissolved in aqueous stock solutions. N-ω-Nitro- L-arginine (L-NNA, Tocris Cookson) was dissolved in a stock solution containing 1 mol · l^{-1} HCl before dilution in the 107 mmol · l^{-1} NaCl buffer. Ionomycin was dissolved in ethanol, jasplakinolide (Molecular Probes) in methanol and 1-{6[17ß-3-methoxyestra-1,3,5(10)-trien-17-yl]aminohexyl}-1H-pyrrole-2,5-dion (U-73122; Calbiochem, Bad Soden, Germany) in chloroform. If not indicated differently, drugs were from Sigma (Deisenhofen, Germany).

Statistics

Results are given as means ± one standard error of mean (SEM). In the case that means of several groups had to be compared, an analysis of variance was performed followed by a post-hoc test of Scheffé. For comparison of two groups, either Student's *t*-test or a Mann-Whitney *U*-test was applied. An *F*-test decided which test method had to be used. Both paired and unpaired two-tailed Student's *t*-tests were applied as appropriate. $P < 0.05$ was considered statistically significant.

Results

Carbachol-Induced Decrease in Intracellular Cl^- Concentration under Depolarized Conditions

As the dominant action of carbachol at rat colonic epithelium consists in the opening of basolateral and apical Ca^{2+}-dependent K^+ channels, which causes hyperpolarization of the membrane and thereby indirectly enhances Cl^- efflux via a change in driving force (Böhme et al., 1991; Strabel & Diener, 1995; Schultheiss et al., 2003), all experiments were performed under depolarized conditions, i.e., in the presence of a high extracellular K^+ concentration. When carbachol ($5 \cdot 10^{-5}$ mol · l^{-1}) was administered during superfusion with the 140 mmol · l^{-1} KCl solution, no change in the MEQ signal was observed, as had to be expected due to the missing driving force for Cl^- efflux under these conditions. However, when an outwardly directed Cl^- gradient was applied by superfusion with a 140 mmol · l^{-1} K gluconate solution, a fast increase in the MEQ signal was observed (Fig. 1). As the MEQ fluorescence is quenched by halides (Biwersi & Verkman, 1991), this increase indicates a decrease in the intracellular Cl^- concentration ($\Delta[Cl^-]_i$). When the MEQ fluorescence was calibrated by the use of ionophores and superfusion with solutions of different halide concentrations (*see* "Methods"), carbachol evoked a $\Delta[Cl^-]_i$ of 27.6 ± 3.4 mmol · l^{-1} ($P < 0.05$, $N = 5$, $n = 45$). In contrast, when the crypts were superfused solely with a K gluconate solution that did not contain carbachol, only $\Delta[Cl^-]_i$ of 10.6 ± 2.2 mmol · l^{-1} was observed (Fig. 2), indicating that carbachol enhanced Cl^- efflux under depolarized conditions.

The effect of carbachol was mimicked by the Ca^{2+} ionophore ionomycin (10^{-7} mol · l^{-1}, applied in a buffer containing 10 mmol · l^{-1} Ca^{2+} in order to favor the ionophore-carried Ca^{2+} influx), which induced a $\Delta[Cl^-]_i$ of

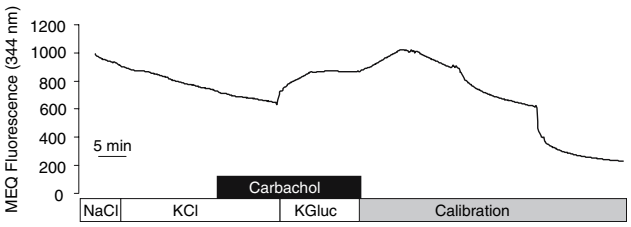

Fig. 1 Increase in MEQ fluorescence induced by carbachol ($5 \cdot 10^{-5}$ mol · l^{-1}, *black bar*) during superfusion under depolarized conditions (high-K^+ buffers) and in the presence of an outwardly directed Cl^- gradient (superfusion with 140 mmol · l^{-1} K gluconate buffer). At the end of the experiment, the MEQ signal was calibrated by superfusion with three different solutions with different halide concentrations in the presence of ionophores (see "Methods"). Typical tracing from $n = 45$ cells from $N = 5$ crypts; for statistics, see Figure 2

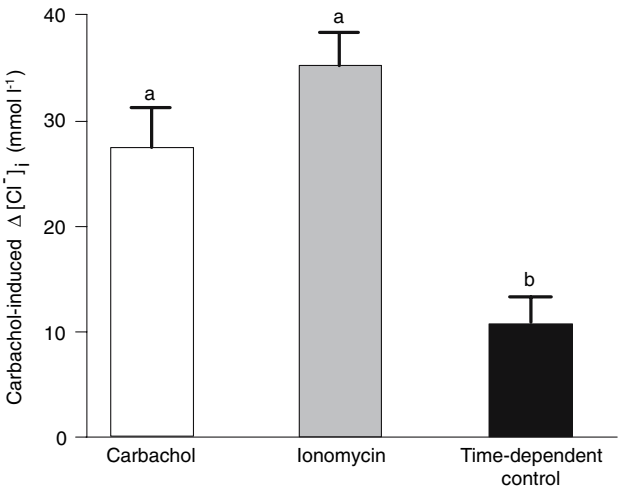

Fig. 2 Decrease of $[Cl^-]_i$ evoked by carbachol ($5 \cdot 10^{-5}$ mol · l^{-1}, *white bar*) or ionomycin (10^{-7} mol · l^{-1} in the presence of 10^{-2} mol · l^{-1} Ca^{2+}, *gray bar*) compared to a time-dependent control (*black bar*). Statistically homogenous groups are indicated by identical letters (analysis of variances followed by test of Scheffé). Values are means ± SEM from $n = 42$–57 cells from $N = 5$ crypt preparations

similar amplitude and time course compared to carbachol (Fig. 2).

The response to carbachol was not dependent on the localization of the cell along the longitudinal axis of the crypt. The cholinergic agonist evoked a similar (and statistically homogenous) decrease in $[Cl^-]_i$ in the fundus region of the crypt, where the most undifferentiated cells are located (Lipkin, 1987); the middle region; as well as near the surface, with its highly differentiated mature enterocytes (Fig. 3). Therefore, in all experiments, data from different regions of the crypt were pooled.

In depolarized rat colonic mucosa, the carbachol-induced Cl^- current across the apical membrane is inhibited by stilbenes (Schultheiss et al., 2005), known blockers of Ca^{2+}-dependent Cl^- channels (Nilius & Droogmans, 2003). Consequently, the sensitivity of the carbachol effect at MEQ-loaded crypts against these drugs was tested. Due to the fluorescence properties of the stilbenes, no calculation of the changes in intracellular Cl^- concentration were performed for these series of experiments; instead, only the changes in MEQ fluorescence intensity were quantified. The stilbene SITS (10^{-3} mol · l^{-1}) inhibited about half of the increase in the MEQ signal evoked by carbachol (Fig. 4), whereas another stilbene, DIDS (10^{-4} mol · l^{-1}), completey prevented any increase in the MEQ signal induced by carbachol during superfusion with the K gluconate solution (Fig. 4).

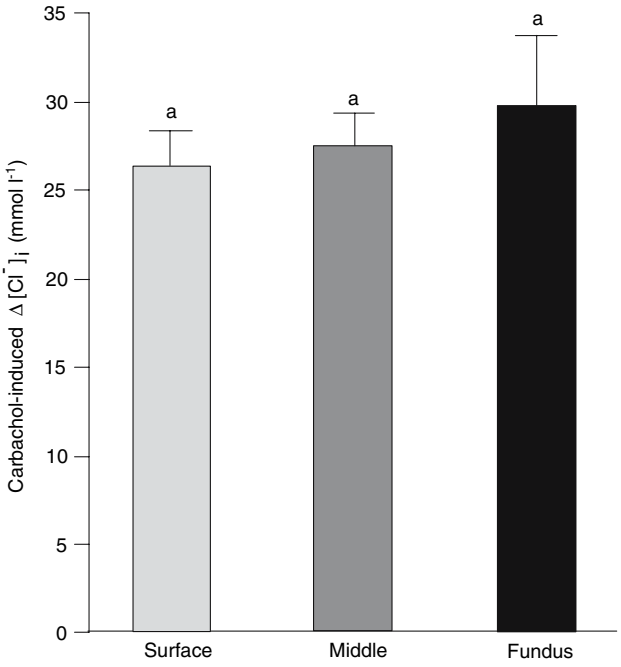

Fig. 3 Decrease of $[Cl^-]_i$ evoked by carbachol ($5 \cdot 10^{-5}$ mol · l^{-1}, *white bar*) at the surface region of the crypt (*left bar*), in the middle region (*middle bar*) and at the fundus region (*right bar*). Statistically homogenous groups are indicated by identical letters; i.e., no significant differences between the three groups were observed (analysis of variances followed by test of Scheffé). Values are means ± SEM from $n = 57$–93 cells from $N = 5$–8 crypt preparations

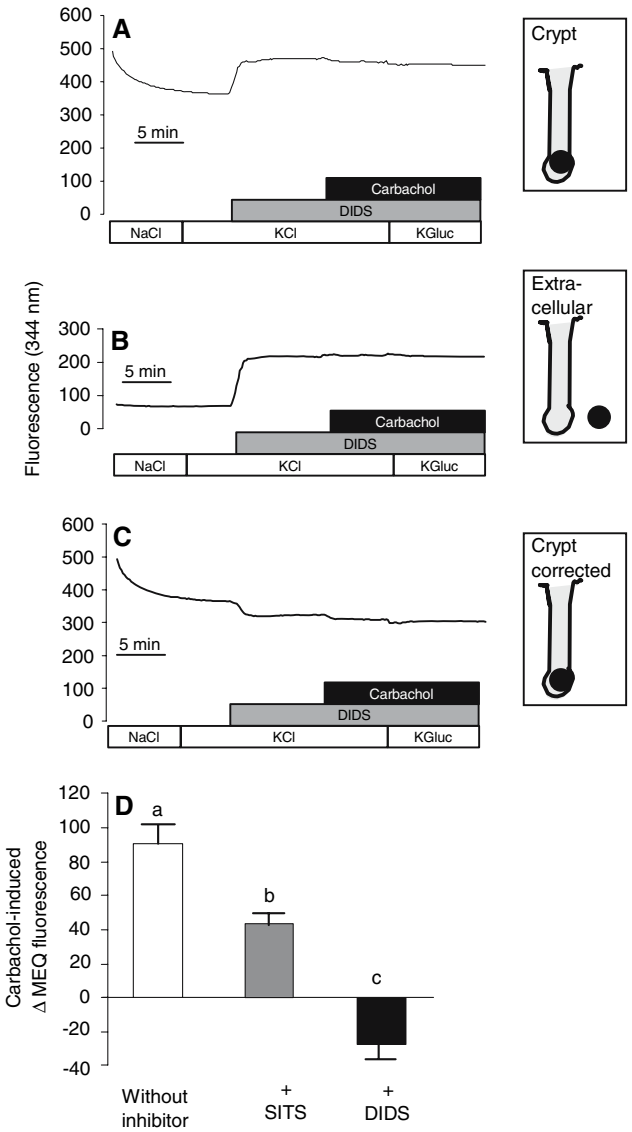

Fig. 4 Missing effect of carbachol ($5 \cdot 10^{-5}$ mol · l^{-1}, *black bar*) on the fluorescence signal of MEQ-loaded crypts in the presence of DIDS (10^{-4} mol · l^{-1}, *gray bar*) (**a**). The paradoxical increase in the fluorescence after administration of DIDS is caused by the fluorescence properties of the stilbene as shown by synchronous measurement in a region of interest outside the crypt, indicated by the schematic drawing (**b**). When this increase in fluorescence after administration of DIDS is subtracted, a decrease in the MEQ fluorescence in the epithelium can be seen (**c**). **d** Mean values of carbachol-induced change in MEQ-fluorescence in the absence of inhibitors (*white bars*), in the presence of SITS (10^{-3} mol · l^{-1}, *gray bar*) or in the presence of DIDS (10^{-4} mol · l^{-1}, *black bar*). Due to the fluorescence properties of the stilbenes, no calculation of the changes in intracellular Cl^- concentrations was performed. Statistically homogenous groups are indicated by identical letters (analysis of variances followed by test of Scheffé). Values are means ± SEM from $n = 46$–77 cells from $N = 5$ crypt preparations

Sensitivity against Inhibitors of Classical Ca^{2+} Signaling Cascades

Classical signaling cascades stimulated by muscarinic receptors of the M_1, M_3 or M_5 type involve stimulation of phospholipase C, leading to the production of inositol 1,4,5-trisphosphate (IP_3) and the release of stored Ca^{2+} (Caulfield & Birdsall, 1998). The final consequences are in general activation of protein kinase(s) C and/or calmodulin, which are in many cases responsible for the modulation of target proteins such as ion channels or transporters (Abdel-Latif, 1986).

Therefore, the ability of typical inhibitors of these signaling cascades to interfere with the carbachol-induced Cl^- efflux was tested. Neither calmidazolium (10^{-6} mol $\cdot$ l^{-1}), a calmodulin antagonist (*see*, *e.g.*, Worrell & Frizzell, 1991), nor U-73122 (10^{-5} mol $\cdot$ l^{-1}), a phospholipase C inhibitor (Taylor & Broad, 1998), nor Gö 6983 (10^{-5} mol $\cdot$ l^{-1}), an inhibitor of atypical protein kinases C (*see*, *e.g.*, Chow, Uribe & Barrett, 2000), had any inhibitory action on carbachol-induced $\Delta[Cl^-]_i$ (Fig. 5). Only staurosporine (10^{-6} mol $\cdot$ l^{-1}), an inhibitor of different protein kinases including protein kinase(s) C (Tamaoki et al., 1986), reduced carbachol-induced $\Delta[Cl^-]_i$ by about half ($P < 0.05$, Fig. 5), suggesting that classical Ca^{2+}-signaling pathways play only a minor role in the mediation of this response.

Involvement of Nitric Oxide

Ussing chamber experiments, where apical Ca^{2+}-activated Cl^- currents were studied at basolaterally depolarized tissues, revealed evidence for the ability of nitric oxide (NO) to stimulate this Cl^- conductance (Schultheiss et al., 2005). Therefore, we tested the ability of NO synthase (NOS) blockers to inhibit carbachol-induced $\Delta[Cl^-]_i$. L-NMMA (10^{-4} mol $\cdot$ l^{-1}), a blocker of all known isoforms of NOS including the inducible form NOS-2 (Reif & McCreedy, 1995; Arzumanian et al., 2003), suppressed the carbachol-induced change in $[Cl^-]_i$ to the level of a time-dependent control (Table 1). In contrast, L-NNA (10^{-4} mol $\cdot$ l^{-1}), which inhibits NOS-1 and NOS-3 but has only a weak action on NOS-2 (Dwyer, Bredt & Snyder 1991), was ineffective (Table 1).

Vice versa, a NO donor, SNP (10^{-4} mol $\cdot$ l^{-1}), mimicked the action of carbachol on $[Cl^-]_i$. Superfusion of the crypts with SNP evoked a $\Delta[Cl^-]_i$ of -24.7 ± 3.0 mmol $\cdot$ l^{-1} ($N = 5$, $n = 42$), i.e., a response of similar amplitude (and time course) as the action of carbachol.

NO has been shown to activate also Cl^- channels of the type CFTR (*see, e.g.*, Schultheiss et al., 2002). Therefore, the effect of SNP was tested in the presence of glibenclamide ($5 \cdot 10^{-4}$ mol $\cdot$ l^{-1}), a blocker of this channel (Greger, 2000). Overall, glibenclamide inhibited the action of the NO donor, too. Closer inspection of the data revealed that there were two groups of cells. In one group ($n = 46$ of 72 cells), the CFTR inhibitor completely suppressed the action of carbachol (decrease in $[Cl^-]_i$ of 4.2 ± 0.6 mmol $\cdot$ l^{-1}), whereas in the other group of cells (26 of 72 cells) glibenclamide was nearly ineffective as carbachol induced a decrease in $[Cl^-]_i$ of 23.0 ± 1.6 mmol $\cdot$ l^{-1}. This fits well with previously published Ussing chamber data, which showed that the long-lasting increase in I_{sc} evoked by an NO donor is totally inhibited by the CFTR blocker glibenclamide but that a transient elevation of I_{sc} (which would be in accordance with the activation of a

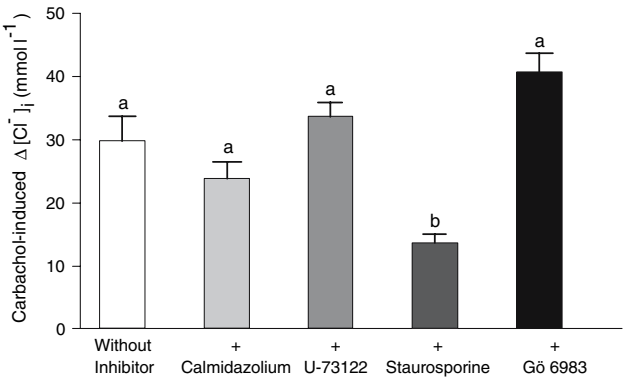

Fig. 5 Effect of inhibitors of Ca^{2+}-signaling cascades on carbachol-induced decrease in $[Cl^-]_i$. Given is the response to carbachol ($5 \cdot 10^{-5}$ mol $\cdot$ l^{-1}) in the absence of any inhibitors or in the presence of calmidazolium (10^{-6} mol $\cdot$ l^{-1}), U-73122 (10^{-5} mol $\cdot$ l^{-1}), staurosporine (10^{-6} mol $\cdot$ l^{-1}) or Gö 6983 (10^{-5} mol $\cdot$ l^{-1}). Statistically homogenous groups are indicated by identical letters (analysis of variances followed by test of Scheffé). Values are means $\pm$ SEM from $n = 46$–75 cells from $N = 4$–6 crypt preparations

Table 1 Effect of putative inhibitors on the carbachol-induced decrease in intracellular Cl^- concentration ($\Delta[Cl^-]_i$)

Inhibitor	Carbachol-induced $\Delta[Cl^-]_i$ (mmol $\cdot$ l^{-1})	*N/n*
No inhibitor	-27.6 ± 3.4	5/45
L-NNA	-33.9 ± 3.0	6/95
L-NMMA	-13.9 ± 2.0*	5/45
Colchicine	-12.2 ± 2.2*	6/70
Nocodazole	-9.8 ± 2.0*	6/44
Jasplakinolide	-14.7 ± 1.8*	5/75
Cytochalasin D	-20.0 ± 1.8	5/83

The effect of carbachol ($5 \cdot 10^{-5}$ mol $\cdot$ l^{-1}) is given in the absence of any inhibitors and in the presence of L-NNA (10^{-4} mol $\cdot$ l^{-1}), L-NMMA (10^{-4} mol $\cdot$ l^{-1}), colchicine ($2.5 \cdot 10^{-5}$ mol $\cdot$ l^{-1}), nocodazole ($3.5 \cdot 10^{-6}$ mol $\cdot$ l^{-1}), jasplakinolide (10^{-6} mol $\cdot$ l^{-1}) or cytochalasin D (10^{-5} mol $\cdot$ l^{-1}). Values are means $\pm$ SEM; n = number of cells from N = number of crypts.

*$P < 0.05$ *vs.* response to carbachol in the absence of any inhibitor (analysis of variance followed by test of Scheffé)

Ca^{2+}-dependent Cl^- conductance) could still be evoked in about half of the tissues after blockade of CFTR (Schultheiss et al., 2002).

If NO should play a role in the activation of Ca^{2+}-evoked Cl^- efflux, the epithelium should possess the ability to produce this gaseous messenger substance; i.e., it should express NO synthases. Therefore, an immunhistochemical study was performed with antibodies against different forms of NOS, from which three isoforms (NOS-1, NOS-2, NOS-3) are known (Knowles & Moncada, 1994). Signals for all three forms could be observed within the colonic epithelium (Fig. 6), with the inducible form, NOS-2, exhibiting the most consistent pattern of expression all over the longitudinal axis of the crypts.

Sensitivity against Drugs Acting on the Cytoskeleton

The different sensitivity of carbachol-induced $\Delta[Cl^-]_i$ against L-NMMA and L-NNA (Table 1) and the predominant staining for NOS-2 in crypt epithelium (Fig. 6) suggest a role for the inducible form of NOS in the mediation of Ca^{2+}-induced, stilbene-sensitive Cl^- efflux. However, in contrast to the two constitutive forms, NOS-1 and NOS-3, NOS-2 is not activated by Ca^{2+} (Knowles & Moncada, 1994). Nevertheless, a rise of the cytosolic Ca^{2+} concentration, as evoked, e.g., by the ionophore ionomycin, is sufficient to induce efflux of Cl^- (Fig. 2). Consequently, there should be another link between the rise of the cytosolic Ca^{2+} concentration and the activation of NOS. One possible candidate is the cytoskeleton, which is known to interact with and to regulate different forms of NOS (Glynne et al., 2002; Su, Zharikov & Block, 2002; Kondrikov et al., 2006) and which itself is affected by cytosolic Ca^{2+} (*see*, *e.g.*, Li, Guan, & Chien, 2005). Therefore, the ability of drugs that interfere with actin and microtubuli with carbachol-induced $\Delta[Cl^-]_i$ was tested.

Colchicine ($2.5 \cdot 10^{-5}$ mol $\cdot$ l^{-1}), a drug that induces depolymerization of microtubuli (Schroer & Sheetz, 1990), suppressed the activation of Cl^- efflux by carbachol (Table 1). A similar inhibition was observed with nocodazole ($3.5 \cdot 10^{-6}$ mol $\cdot$ l^{-1}), a chemically nonrelated compound with similar biological actions as colchicine (Table 1).

In order to confirm this observation, Ussing chamber experiments were performed at basolaterally depolarized colonic epithelia with a Cl^- concentration gradient to drive a Cl^- current across the apical membrane. Under these conditions, carbachol stimulates a transient, stilbene-sensitive Cl^- current, which is followed by a long-lasting inhibition, probably of the CFTR channel as dominant apical Cl^- channel (Schultheiss et al., 2005). The stimulation of Cl^- current (marked by an arrow in Fig. 7) was inhibited by about 90% in the presence of colchicine ($2.5 \cdot 10^{-5}$ at the serosal side, Table 2).

Also, drugs that interfere with the actin cytoskeleton reduced carbachol-evoked $\Delta[Cl^-]_i$. Jasplakinolide (10^{-6} mol $\cdot$ l^{-1}), which strengthens the actin cytoskeleton by stabilization of F-actin (*see*, *e.g.*, Ahmed et al., 2000), inhibited carbachol-evoked $\Delta[Cl^-]_i$ even more strongly than the microtubule blockers (Table 1). In contrast, cytochalasin D (10^{-5} mol $\cdot$ l^{-1}), which blocks the polymerization of actin (Lin et al., 1980), was ineffective (Table 1).

Immunhistochemical Detection of Bestrophin, a Candidate for Ca^{2+}-Dependent Cl^- Channels

The molecular nature of Ca^{2+}-dependent Cl^- channels is still not clear. However, recent experiments suggest the possible involvement of bestrophins (Pifferi et al., 2006). Consequently, we investigated by immunhistochemistry whether the rat colonic epithelium expresses this protein using a polyclonal antibody which had already been successfully applied at the proximal mouse colon (Puntheeranurak et al., 2007). Indeed, the experiments demonstrated strong labeling of all epithelial cells along the crypt axis (Fig. 8), indicating that this candidate protein for Ca^{2+}-dependent Cl^- channels is present in this tissue.

Discussion

The present results demonstrate that carbachol, which evokes an increase in the cytoplasmic Ca^{2+} concentration of colonic enterocytes (Lindqvist et al., 1998), as well as the Ca^{2+} ionophore ionomycin evoke a Cl^- efflux at rat colonic crypts loaded with the halide-sensitive fluorescent dye MEQ under depolarized conditions (Figs. 1, 2). Membrane potential reaches 0 m*V* when crypt cells are superfused with high-K^+ buffers (Schultheiss & Diener, 1998). Therefore, the opening of Ca^{2+}-dependent K^+ channels, which is the main effect of carbachol under nondepolarized conditions (Böhme et al., 1991), can no longer indirectly favor Cl^- secretion via hyperpolarization of the membrane as the membrane potential is already clamped at the reversal potenial for K^+ under these conditions and can no longer be hyperpolarized by a further increase in K^+ conductance. However, this strategy cannot completely rule out the possibility that an opening of Ca^{2+}-dependent apical and basolateral K^+ channels might still favor Ca^{2+}-induced Cl^- efflux as this would allow the enhanced efflux of a counter ion for each secreted Cl^- anion. However, this efflux was sensitive against stilbenes such as SITS and DIDS (Fig. 4), known inhibitors of Ca^{2+}-dependent Cl^- channels (Nilius & Droogmans, 2003).

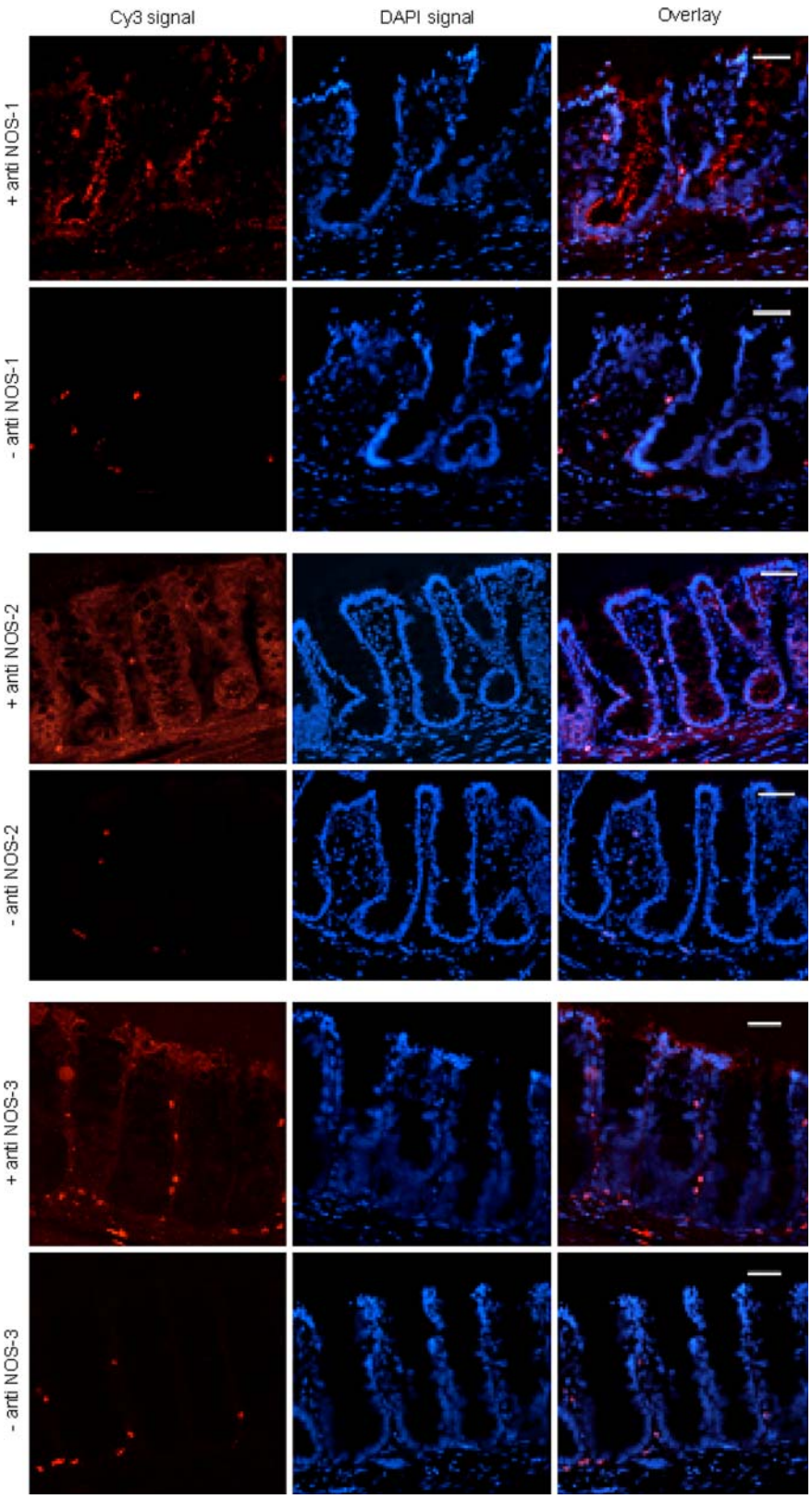

Fig. 6 Immunohistochemical staining against NOS-1 (*rows 1* and *2*), NOS-2 (*rows 3* and *4*) or NOS-3 (*rows 5* and *6*) in rat colonic wall. The orientation of each picture is as follows: *lower part*, muscularis mucosae; *upper part*, surface region of the colonic epithelium. *Left column*, NOS signal (Cy3-labeled, *red*); *middle column*, nuclear staining with DAPI (*blue*); *right column*, overlay of both. *Rows 1, 3* and *5*, labeling; *rows 2, 4* and *6*, negative control without primary antibody against the corresponding NOS. Scale bars = 50 μm

These drugs interfere also with other anion transporters, especially with the Cl^-/HCO_3^- exchanger(s) responsible for intestinal Cl^- absorption. However, all experiments were carried out in the absence of HCO_3^-, and cholinergic agonists inhibit Cl^- absorption (measured as unidirectional mucosal-to-serosal flux) instead of activating it (Zimmerman,

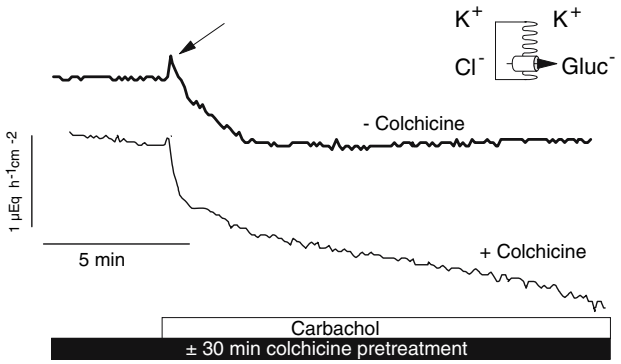

Fig. 7 Effect of carbachol ($5 \cdot 10^{-5}$ mol $\cdot$ l^{-1}at the serosal side, *white bar*) on Cl^- current across apical Cl^- channels in the absence (*upper thick line*) and presence (*lower thin line*) of colchicine ($2.5 \cdot 10^{-5}$ mol $\cdot$ l^{-1} for 30 min). Tissues were basolaterally depolarized (111.5 mmol $\cdot$ l^{-1} KCl at the serosal side) in the presence of a Cl^- gradient (107 mmol $\cdot$ l^{-1} Kgluconate/4.5 mmol $\cdot$ l^{-1} KCl at the mucosal side) as indicated by the schematic *inset*. A positive I_{sc} indicates the transport of anions from the serosal to the mucosal side (or the transport of cations in the reverse direction). Carbachol evokes a transient increase in I_{sc} under control conditions, as indicated by the *arrow*. Typical tracings for eight or nine experiments under each condition; for statistics, see Table 2

Table 2 Effect of colchicine on Cl^- current across the apical membrane evoked by carbachol

	ΔI_{sc} evoked by carbachol in the presence of the inhibitor	ΔI_{sc} evoked by carbachol in the absence of the inhibitor	n
Colchicine (μEq $\cdot$ h^{-1} $\cdot$ cm^{-2})			
ΔI_{sc} peak	0.026 ± 0.019*	0.23 ± 0.086	8–9
ΔI_{sc} 10 min	−1.07 ± 0.13	−1.27 ± 0.14	8–9

Tissues were basolaterally depolarized (111.5 mmol $\cdot$ l^{-1} KCl at the serosal side) in the presence of a serosally to mucosally directed Cl^- gradient (107 mmol $\cdot$ l^{-1} K gluconate/4.5 mmol $\cdot$ l^{-1} KCl mucosal bathing solution). Drug concentrations were carbachol ($5 \cdot 10^{-5}$ mol $\cdot$ l^{-1} at the serosal side), colchicine ($2.5 \cdot 10^{-5}$ at the serosal side, administered 30 min before administration of carbachol). The values represent the maximal carbachol-induced I_{sc} (peak) as well as the long-lasting decrease in I_{sc}, measured 10 min after administration of carbachol (I_{sc} 10 min). Values are given as difference from the baseline just prior to administration of the cholinergic agonist (ΔI_{sc}) and are means ± SEM.

*$P < 0.05$ *vs.* carbachol response in the absence of the respective inhibitor. Baseline I_{sc} just prior to administration of carbachol amounted to −1.72 ± 0.24 μEq $\cdot$ h^{-1} $\cdot$ cm^{-2} in the presence and −1.79 ± 0.14 μEq $\cdot$ h^{-1} $\cdot$ cm^{-2} in the absence of colchicine

Dobbins & Binder, 1982), which makes interference of carbachol with these exchangers in the present experiments unlikely. Possible proteins underlying this efflux might be ClCa channels (Fuller et al., 2001) or bestrophins (Pifferi et al., 2006), which both are expressed at the rat distal colon (Fig. 8; Schultheiss et al., 2005).

Consequently, this Ca^{2+}-induced $\Delta[Cl^-]_i$ seems to reflect activation of the stilbene-sensitive apical Cl^- conductance previously observed in Ussing chamber experiments (Schultheiss et al., 2005), although some differences seem to exist between the two experimental systems. For example, at isolated crypts, DIDS is a very potent blocker of carbachol-evoked $\Delta[Cl^-]_i$ (Fig. 4), whereas in Ussing chamber experiments DIDS was less effective than SITS at inhibiting carbachol-stimulated apical Cl^- current (Schultheiss et al., 2005). This discrepancy might indicate that the more lipophilic compound, DIDS, which possesses a 4-isothiocyanato group instead of the 4-acetamido group of SITS, might have limited access in the Ussing chamber to its presumed target site, i.e., apical Cl^- channels, as the mucus layer covering the mucosa might be an efficient diffusion barrier. Also, the time course of the carbachol-induced apical I_{sc} differs from that of the change of the cytoplasmic Cl^- concentration as it is more rapidly down-regulated; i.e., it disappears in about 1 min (Fig. 7), whereas the carbachol-induced $\Delta[Cl^-]_i$ lasts for at least 5 min, before $[Cl^-]_i$ stabilizes at a new value (Fig. 1). A possible reason for this discrepancy might be the different temperature at which both types of experiments were performed, 37°C for the Ussing chamber experiments and room temperature for the MEQ experiments, which may slow down the inactivation of the corresponding Ca^{2+}-dependent Cl^- conductance. Furthermore, the second phase of the carbachol response in the Ussing chamber is thought to be caused by the inhibition of apical CFTR, leading to a decrease in I_{sc} across apical Cl^- channels (Fig. 7). However, CFTR channels have to be in an open state to observe this inhibition, which is in intact tissue caused by the continuous stimulation of cytosolic cAMP production by submucosal production of prostaglandins and/or release of secretory neurotransmitters from the submucosal plexus (Strabel & Diener, 1995), both of which are missing in the isolated crypt model.

The carbachol-induced $\Delta[Cl^-]_i$ is not mediated by typical Ca^{2+} signaling cascades such as the phopholipase C or calmodulin pathway as typical blockers of these pathways were ineffective at inhibiting the carbachol response (Fig. 5). These data confirm previous observations about carbachol-induced Cl^- current across the apical membrane, which had proven to be resistant against, e.g., phospholipase C, IP_3 receptor and calmodulin inhibition (Schultheiss et al., 2005). However, as also observed during these Ussing chamber experiments, the carbachol response was inhibited by NOS blockade (Table 1) and mimicked by the NO donor SNP.

The colonic epithelium is equipped with enzymes to produce NO, i.e., NO synthases. Immunohistochemical staining with antibodies against the three known isoforms of NOS revealed a signal for all isoforms, with the staining

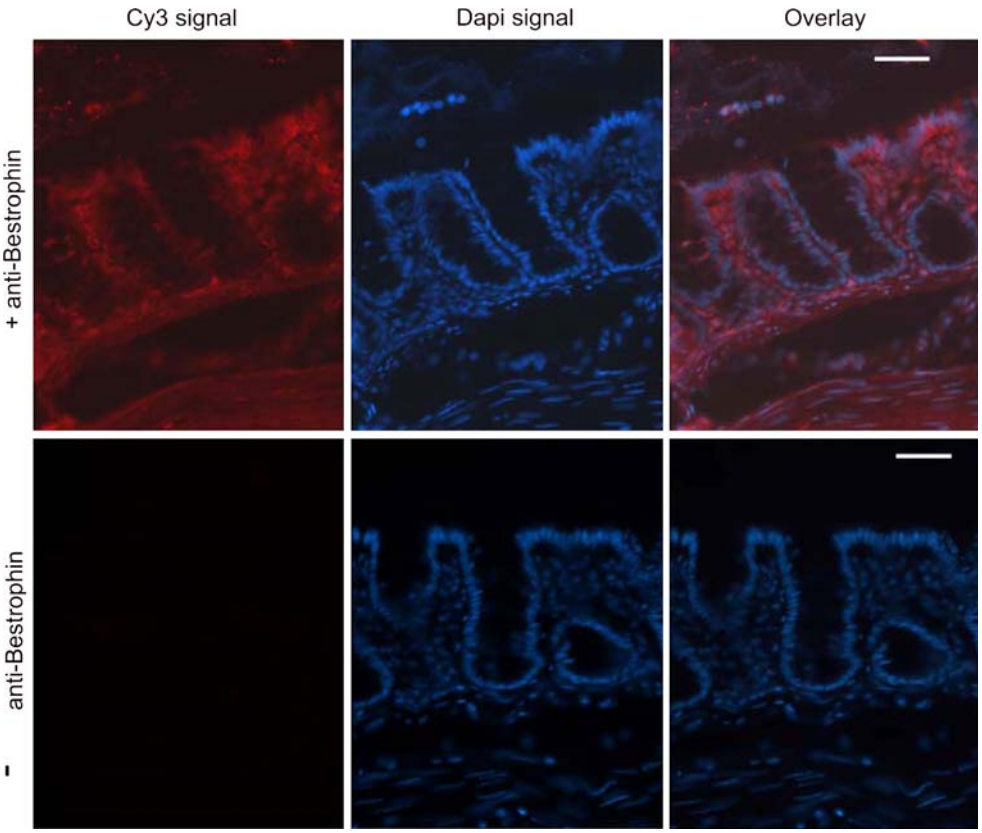

Fig. 8 Immunohistochemical staining against bestrophin in rat colonic wall. The orientation of each picture is as follows: *lower part*, muscularis mucosae; *upper part*, surface region of the colonic epithelium. *Left column*, Bestrophin signal (Cy3-labeled, *red*); *middle column*, nuclear staining with DAPI (*blue*); *right column*, overlay of both. *Row 1*, labeling; *row 2*, negative control without primary antibody against bestrophin. Scale bars = 50 μm

for NOS-2 being most equally distributed along the longitudinal axis of the crypts (Fig. 6). Also, epithelial cells from other origins are known to express NOS-1 (*see*, *e.g.*, Garcia-Vitoria et al., 2000), NOS-2 (Roberts et al., 2001), NOS-3 (Zhan, Li & Johns, 2003) or combinations of them (Puhakka et al., 2006). Especially in the gut, constitutive expression of the inducible form, NOS-2, has been attributed to continuous stimulation of the epithelium, e.g., with bacterial products such as lipopolysaccharide (Roberts et al., 2001). This isoform gave the most continuous immunohistochemical signal at rat colonic epithelium (Fig. 6). Furthermore, the carbachol-evoked $\Delta[Cl^-]_i$ was inhibited by L-NMMA, a blocker of all isoforms of NOS (Reif & McCreedy, 1995; Arzumanian et al., 2003), whereas L-NNA (10^{-4} mol $\cdot$ l^{-1}), which inhibits NOS-1 and NOS-3 but has only a weak action on NOS-2 (Dwyer, Bredt & Snyder 1991), was ineffective (Table 1). Only a 100 times higher concentration of L-NNA is able to inhibit carbachol-evoked Cl^- current across the apical membrane in intact tissue (Schultheiss et al., 2005), suggesting a role for NOS-2 in the mediation of Ca^{2+}-evoked Cl^- efflux.

NOS-2, which seems to be the most likely NOS isoform involved in carbachol-induced $\Delta[Cl^-]_i$, is not directly activated by an increase in the cytosolic Ca^{2+} concentration (Knowles & Moncada, 1994). Therefore, other mechanisms have to be considered for how a NOS might be involved in the activation of stilbene-sensitive Cl^- efflux. NOSs are known to interact with the cytoskeleton. For human proximal tubular cells and other epithelia, an interaction of NOS-2 with actin via PDZ-domain interaction with ezrin has been demonstrated (Glynne et al., 2002). For porcine endothelium, NOS activity has been shown to be regulated by microtubuli (Su et al., 2002) as well as by actin, for which direct interactions seem to exist (Kondrikov et al., 2006). Also, at rat colon, the carbachol-evoked $\Delta[Cl^-]_i$ could be inhibited by drugs such as nocodazole and colchicine (Table 1), inducing depolymerization of microtubuli. Jasplakinolide, leading to the stabilization of F-actin, was effective, too (Table 1), suggesting that both a functional microtubular network as well as a functional actin cytoskeleton are necessary for the activation of cholinergic-induced Cl^- efflux. The mechanisms and the presumed changes in the cytoskeleton of the rat colonic epithelium induced by cholinergic stimulation must be clarified in future experiments.

In conclusion, these results demonstrate the presence of a stilbene-sensitive, Ca^{2+}-dependent Cl^- efflux pathway all along the crypt axis. Its physiological contribution to colonic Cl^- secretion, compared to the contribution of the CFTR channel, is probably quite small because Ca^{2+}-induced Cl^- currents can only be measured when the predominant action of cytosolic Ca^{2+} on Ca^{2+}-dependent K^+ currents is suppressed by the use of high-K^+ solutions (Schultheiss et al., 2005). However, it might become significant in diseases such as cystic fibrosis, where some

patients can develop Cl^- conductances other than CFTR (Bronsveld et al., 2000). Both NO as well as the cytoskeleton play a role during its activation. Consequently, NO, continuously produced by the epithelium, not only regulates small intestinal solute transporter such as the Na^+-dependent glucose transporter SGLT-1 (Coon et al., 2005) but also seems to play a role in the regulation of colonic ion transport.

Acknowledgments The diligent care of B. Brück, E. Haas, A. Metternich and B. Schmidt is a pleasure to acknowledge. This work was supported by Deutsche Forschungsgemeinschaft, grant Di 388/9-1.

References

Abdel-Latif AA (1986) Calcium-mobilizing receptors, polyphosphoionisitides and the generation of second messengers. Pharmacol Rev 38:227–272

Ahmed N, Ramjeesingh M, Wong S, Varga A, Garami E, Bear CE (2000) Chloride channel activity of CIC-2 is modified by the actin cytoskeleton. Biochem J 352:789–794

Arzumanian V, Stankevicius E, Laukeviciene A, Kevelaitis E (2003) Mechanisms of nitric oxide synthesis and action in cells. Medicina 39:535–541

Barrett KE, Smitham J, Traynor-Kaplan A, Uribe JM (1998) Inhibition of Ca^{2+}-dependent Cl^- secretion in T84 cells: membrane target(s) of inhibition is agonist specific. Am J Physiol 274:C958–C965

Binder HJ, Sandle GI (1994) Electrolyte transport in the mammalian colon. In: Johnson LR (ed) Physiology of the gastrointestinal tract. Raven Press, New York, pp 2133–2171

Biwersi J, Verkman AS (1991) Cell-permeable fluorescent indicator for cytosolic chloride. Biochemistry 30:7879–7883

Böhme M, Diener M, Rummel W (1991) Calcium- and cyclic-AMP-mediated secretory responses in isolated colonic crypts. Pfluegers Arch 419:144–151

Bronsveld I, Mekus F, Bijman J, Ballmann M, Greipel J, Hundrieser J, Halley DJJ, Laabs U, Busche R, De Jonge HR, Tümmler B, Veeze HJ (2000) European CF Twin and Sibling study consortium. Residual chloride secretion in intestinal tissue of deltaF508 homozygous twins and siblings with cystic fibrosis. Gastroenterology 119:32–40

Caulfield MP, Birdsall NJM (1998) International Union of Pharmacology. XVII. Classification of muscarinic acetylcholine receptors. Pharmacol Rev 50:279–290

Chow JYC, Uribe JM, Barrett KM (2000) A role for protein kinase C epsilon in the inhibitory effect of epidermal growth factor on calcium-stimulated chloride secretion in human colonic epithelial cells. J Biol Chem 275:21169–21176

Coon S, Kim J, Shao GH, Sundaram U (2005) Na-glucose and Na-neutral amino acid cotransport are uniquely regulated by constitutive nitric oxide in rabbit small intestinal villus cells. Am J Physiol 289:G1030–G1035

Dwyer MA, Bredt DS, Snyder SH (1991) Nitric oxide synthase: irreversible inhibition by L-NG-nitroarginine in brain image and image. Biochem Biophys Res Commun 176:1136–1141

Fuchs W, Larsen EH, Lindemann B (1977) Current-voltage curve of sodium channels and concentration dependence of sodium permeability in frog skin. J Physiol 267:137–166

Fuller CM, Ji HL, Tousson A, Elble RC, Pauli BU, Benos DJ (2001) Ca^{2+}-activated Cl^- channels: a newly emerging anion transport family. Pfluegers Arch 443:S107–S110

Garcia-Vitoria M, Garcia-Corchón C, Rodriguez JA, Garcia-Amigot F, Burrell MA (2000) Expression of neuronal nitric oxide synthase in several cell types of the rat gastric epithelium. J Histochem Cytochem 48:1111–1120

Glynne PA, Darling KE, Picot J, Evans TJ (2002) Epithelial inducible nitric-oxide synthase is an apical EBP50-binding protein that directs vectorial nitric oxide output. J Biol Chem 277:33132–33138

Greger R (2000) Role of CFTR in the colon. Annu Rev Physiol 62:467–491

Jentsch TJ, Stein V, Weinreichz F, Zdebik AA (2002) Molecular structure and physiological function of chloride channels. Physiol Rev 82:503–568

Knowles RG, Moncada S (1994) Nitric oxide synthases in mammals. Biochem J 298:249–258

Kondrikov D, Han HR, Block ER, Su Y (2006) Growth and density-dependent regulation of NO synthase by the actin cytoskeleton in pulmonary artery endothelial cells. Am J Physiol 290:L41–L50

Li S, Guan JL, Chien S (2005) Biochemistry and biomechanics of cell motility. Annu Rev Biomed Eng 7:105–150

Lin DC, Tobin KD, Grumet M, Lin S (1980) Cytochalasins inhibit nuclei-induced actin polymerisation by blocking filament elongation. J Cell Biol 84:455–460

Lindqvist SM, Sharp P, Johnson IT, Satoh Y, Williams MR (1998) Acetylcholine-induced calcium signaling along the rat colonic crypt axis. Gastroenterology 115:1131–1143

Lipkin M (1987) Proliferation and differentiation of normal and diseased gastrointestinal cells. In: Johnson LR (ed) Physiology of the gastrointestinal tract. Raven Press New York, pp 255–284

MacVinish LJ, Reancharoen T, Cuthbert AW (1993) Kinin-induced chloride permeability changes in colony 29 epithelia estimated from $^{125}I^-$ efflux and MEQ fluorescence. Br J Pharmacol 108:469–478

Nilius BT, Droogmans G (2003) Amazing chloride channels: an overview. Acta Physiol Scand 177:119–147

Pifferi S, Pascarella G, Boccaccio A, Mazzatenta A, Gustincich S, Menini A, Zucchelli S, (2006) Bestrophin-2 is a candidate calcium-activated chloride channel involved in olfactory transduction. Proc Natl Acad Sci USA 103:12929–12934

Puhakka AR, Harju TH, Paakko PK, Soini YM, Kinnula VL (2006) Nitric oxide synthases are associated with bronchial dysplasia. Lung Cancer 51:275–282

Puntheeranurak S, Schreiber R, Spitzner M, Ousingsawat J, Krishnamra N, Kunzelmann K (2007) Control of ion transport in mouse proximal and distal colon by prolactin. Cell Physiol Biochem 19:77–88

Reif DW, McCreedy SA (1995) *N*-Nitro-L-arginine and *N*-monomethyl-L-arginine exhibit a different pattern of inactivation toward the three nitric oxide synthases. Arch Biochem Biophys 320:170–176

Roberts PJ, Riley GP, Morgan K, Miller R, Hunter JO, Middleton SJ (2001) The physiological expression of inducible nitric oxide synthase (iNOS) in the human colon. J Clin Pathol 54:293–297

Schroer TA, Sheetz MP (1990) Functions of microtubule-based motors. Annu Rev Physiol 53:629–652

Schultheiss G, Diener M (1998) Inhibition of a K^+ conductance by the phosphatase inhibitor calyculin A in rat distal colon. Eur J Pharmacol 349:89–95

Schultheiss G, Ribeiro R, Diener M (2001) Fatty acids inhibit anion secretion in rat colon: apical and basolateral action sites. Pfluegers Arch 442:603–613

Schultheiss G, Seip G, Kocks SL, Diener M (2002) Ca^{2+}-dependent and Ca^{2+}-independent Cl^- secretion stimulated by the nitric oxide donor, GEA 3162, in rat colonic epithelium. Eur J Pharmacol 444:21–30

Schultheiss G, Ribeiro R, Schäfer KH, Diener M (2003) Activation of apical K^+ conductances by muscarinic receptor stimulation in rat

distal colon: fast and slow components. J Membr Biol 195:183–196

Schultheiss G, Siefjediers A, Diener M (2005) Muscarinic receptor stimulation activates a Ca^{2+}-dependent Cl^- conductance in rat distal colon. J Membr Biol 204:117–127

Strabel D, Diener M (1995) Evidence against direct activation of chloride secretion by carbachol in the rat distal colon. Eur J Pharmacol 274:181–191

Su Y, Zharikov SI, Block ER (2002) Microtubule-active agents modify nitric oxide production in pulmonary artery endothelial cells. Am J Physiol 282:L1183–L1189

Tamaoki T, Nomoto H, Takahashi I, Kato Y, Morimoto M, Tomita P (1986) Staurosporine, a potent inhibitor of phospholipid/Ca^{++} dependent protein kinase. Biochem Biophys Res Commun 135:397–402

Taylor CW, Broad LM (1998) Pharmacological analysis of Ca^{2+} signalling: problems and pitfalls. Trends Pharmacol Sci 19:370–375

Warhurst G, Higgs NB, Tonge A, Turnberg LA (1991) Stimulatory and inhibitory actions of carbachol on chloride secretory responses in human colonic cell line T84. Am J Physiol 261:G220–G228

Worrell RT, Frizzell RA (1991) CaMKII mediates stimulation of chloride conductance by calcium in T84 cells. Am J Physiol 260:C877–C882

Zhan X, Li D, Johns RA (2003) Expression of endothelial nitric oxide synthase in ciliated epithelia of rats. J Histochem Cytochem 51:81–87

Zimmerman TW, Dobbins JW, Binder HJ (1982) Mechanism of cholinergic regulation of electrolyte transport in rat colon in vitro. Am J Physiol 242:G116–G123